

## 22.0 Atomic Resonance and Scattering

### Academic and Research Staff

Prof. D. Kleppner, Prof. D.E. Pritchard, Dr. S. Vianna, Dr. J. Derouard, Dr. A. Martin, Dr. G.P. Lafyatis, Dr. R. Ahmad-Bitar, Dr. T.W. Ducas

### Graduate Students

E. Raab, R. Ahmad-Bitar, V. Bagnato, M.M. Kash, C.H. Lu, G.R. Welch, B. Hughey, T. Gentile, E. Hilfer, R.W. Flanagan, R. Hulet, P.J. Martin, A.H. Miklich, P. Magill, B. Oldaker, R. Stoner, E. Cornell, B. Stewart, S. Paine, R. Weiskoff

## 22.1 Basic Atomic Physics

### 22.1.1 Rydberg Atoms in a Magnetic Field

*National Science Foundation (Grant PHY 83-06273)*

Michael M. Kash, George R. Welch, Chun-Ho Lu, Daniel Kleppner

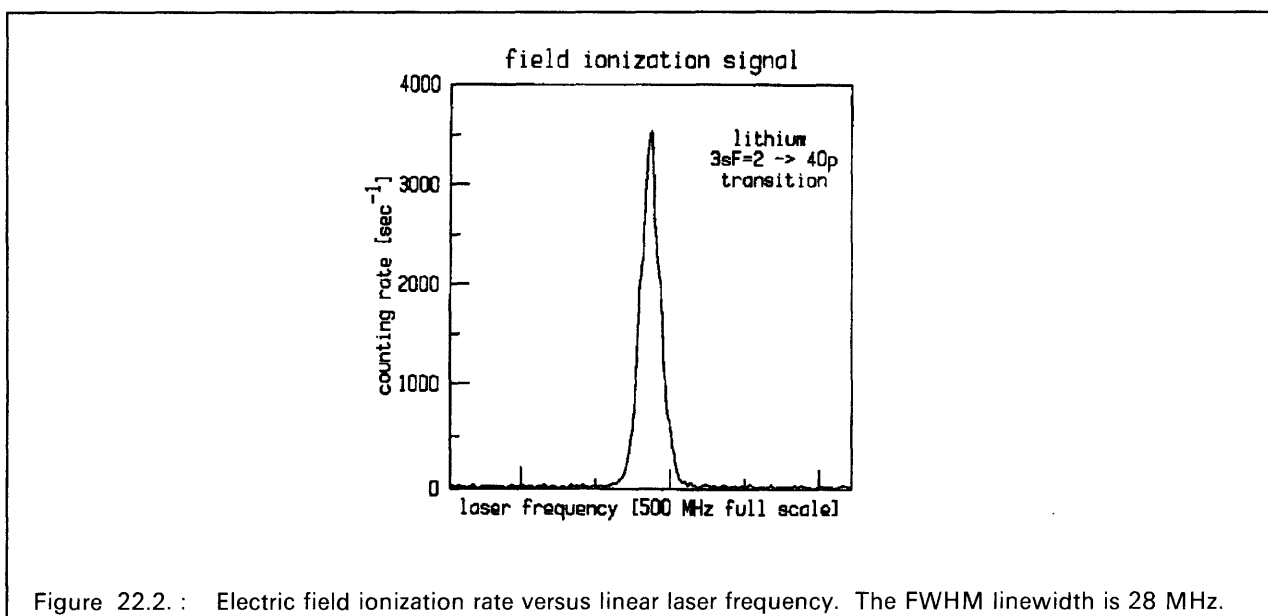
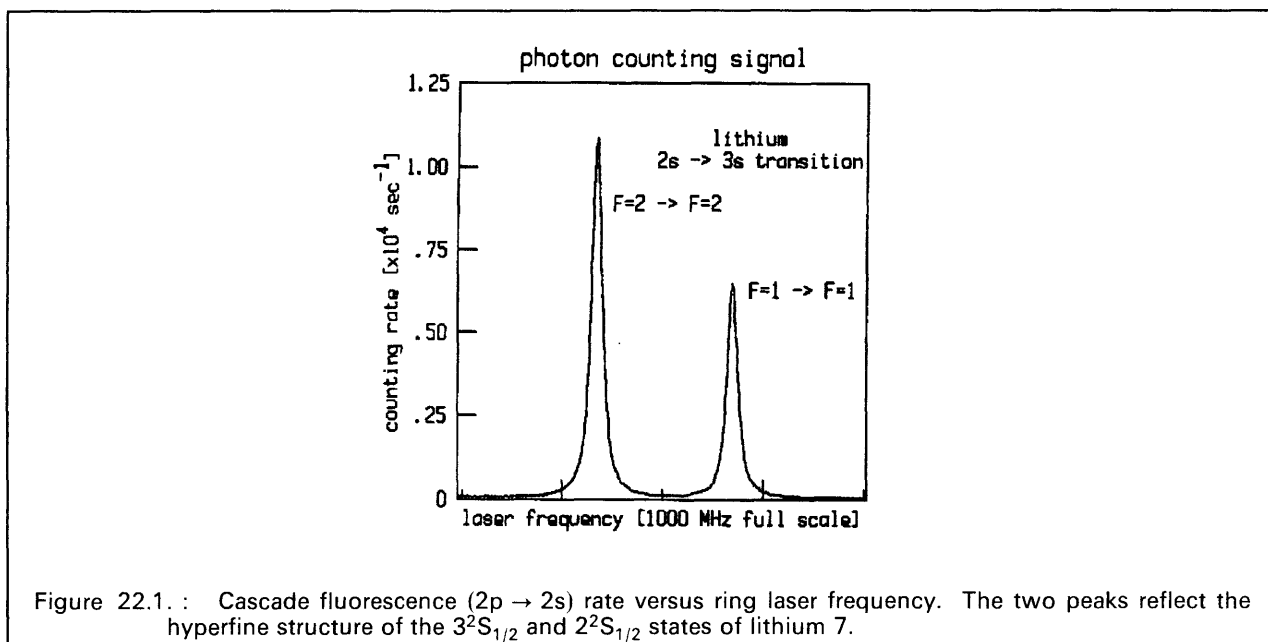
We have produced Rydberg atoms in a lithium atomic beam using cw dye lasers, and developed the technology for detecting these atoms with electric field ionization. These advances have brought us close to the point where we can start carrying out high resolution measurements on highly excited atoms in a strong magnetic field by cw laser spectroscopy.

Understanding the diamagnetic spectrum of an atom with a single valence electron presents a formidable challenge to theory and experiment.<sup>1</sup> The classical and quantum mechanical equations of motion are easily constructed, but in spite of the simplicity of the problem the solutions are elusive and our understanding is far from complete.

Numerical techniques have been applied to both the classical<sup>2</sup> and quantum<sup>3</sup> dynamics, but the results possess features which are difficult to interpret. Construction of an approximate constant of motion is a promising method for predicting the spectrum of a hydrogen atom in a uniform magnetic field.<sup>4</sup> Our primary task is to measure the level anticrossing sizes and linewidths in the diamagnetic spectrum of atomic lithium, for these can establish the credibility of such an operator.<sup>5</sup>

The excitation of lithium Rydberg atoms is performed with a two-step, three-photon process. The first step is a two-photon transition from the 2s state to the 3s state. This step is detected by observing the cascade fluorescence ( $3s \rightarrow 2p$ ,  $2p \rightarrow 2s$ ) through a fiber optic bundle with a sensitive photomultiplier tube. The transition is excited by 735 nm light from a Coherent ring dye laser. The  $2p \rightarrow 2s$  fluorescence as a function of ring laser frequency is shown in Fig. 22.1. The ring laser is stabilized against slow drift by locking to the larger peak's center. The second step is a one-photon transition from the 3s state to the np state. This is observed by counting electrons which are produced in ionizing the excited atoms as they move from the interaction volume into a region of static electric field, 5-10 kV/cm. The electrons are counted with a surface barrier diode.

Standard devices such as electron multiplier tubes, channelrod multipliers, or micro-channel plates do not operate in a strong magnetic field greater than 1 Tesla. Figure 22.2 illustrates the electron counting rate versus linear laser frequency, near the  $3s \rightarrow 4p$  transition. The FWHM linewidth of 28 MHz represents an important advance in Rydberg atom spectroscopy.



To minimize the electric field in the atom's rest frame, the atomic beam of lithium is parallel to the axis of a solenoid superconductive magnet. The interaction region consists of an aluminum cylinder whose axis is parallel to the atomic beam. The cylinder also contains prisms to deflect the lasers so that the laser and atom beams intersect at

right angles, to minimize Doppler broadening. The interaction region combines efficient collection of cascade fluorescence with good geometric rejection of scattered laser light.

We expect to energize the magnet in the near future.

## References

- <sup>1</sup> J.C. Gay, "High-Magnetic Field Atomic Physics," in Progress in Atomic Spectroscopy, edited by H.J. Beyer, H. Kleinpoppen, New York: Plenum, 1984.
- <sup>2</sup> J. Delos, S.K. Knudson and D.W. Nord, Phys. Rev. A *30*, 1208 (1984).
- <sup>3</sup> J.C. Castro, M.L. Zimmerman, R.G. Hulet, D. Kleppner and R.R. Freeman, Phys. Rev. Lett. *45*, 1780 (1980).
- <sup>4</sup> D.R. Henick, Phys. Rev. A *26*, 323 (1982).
- <sup>5</sup> M.L. Zimmerman, M.M. Kash and G.R. Welch, J. Phys. Colloq. C2, *43*, 113 (1982).

## 22.2 Rydberg Atoms and Radiation

*U.S. Navy - Office of Naval Research (Contract N00014-79-C-0183)*  
*Joint Services Electronics Program (Contract DAAL03-86-K-0002)*  
*National Science Foundation (Grant PHY 84-11483)*

Barbara Hughey, Thomas Gentile, E. Hilfer, S. Vianna, R.G. Hulet, Daniel Kleppner

### 22.2.1 Inhibited Spontaneous Emission

We have achieved our initial goal in the study of basic radioactive processes using Rydberg atoms - the observation of inhibited spontaneous emission.<sup>1</sup> An experiment has been carried out demonstrating that spontaneous emission can be effectively turned off.<sup>2</sup>

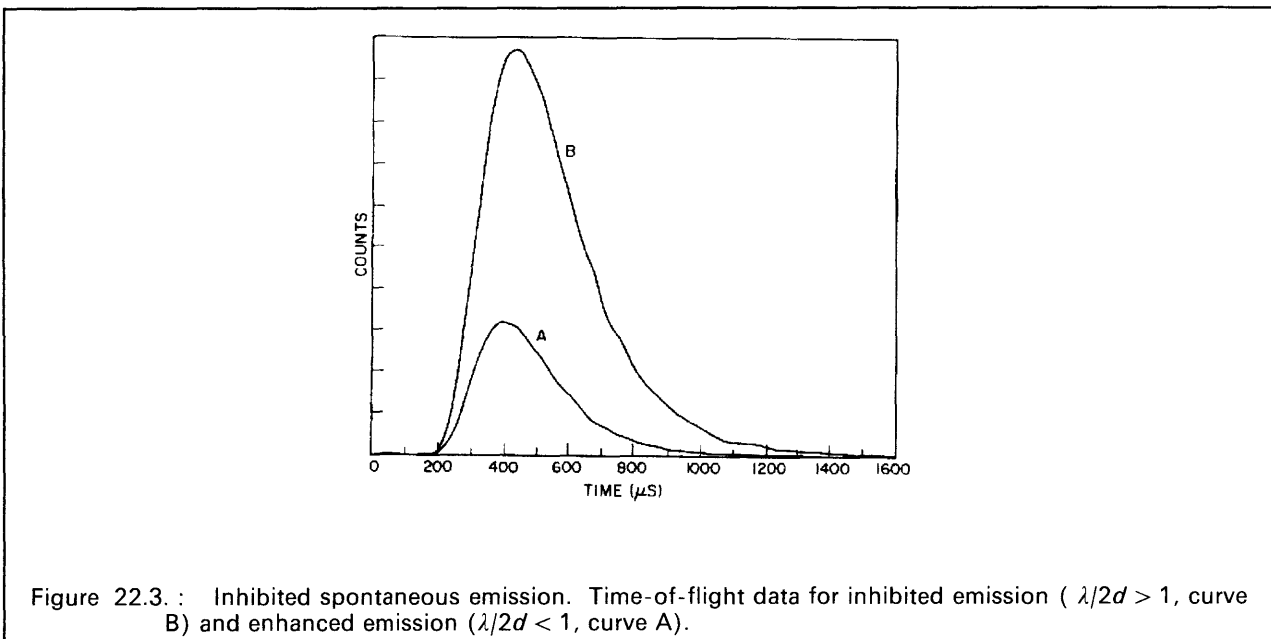
The underlying principle is that spontaneous emission results from the radioactive coupling between matter and a continuum of vacuum states. However, the assumptions underlying the conventional calculation of the density of modes in free space are not always valid. In particular, cavities can dramatically effect spontaneous emission. Such effects are difficult to observe in the optical regime because of the problem of making good fundamental mode cavities at short wavelengths. Excellent cavities can be made at microwave wavelengths, but spontaneous emission is enhanced by a factor of  $n^4$  where  $n$  is the principle quantum number, allowing such effects to be studied.

The experiment involved measuring the natural lifetime (i.e. the inverse of the spontaneous emission rate) for the transition  $n = 23 \rightarrow n = 22$  in cesium. "Circular" Rydberg states were employed.<sup>3</sup> These states have the maximum possible angular momentum  $m = l = n - 1$ ; their value lies in possessing only a single dipole radiation channel. The radiative lifetime was measured by time-of-flight spectroscopy.

Atoms were excited to the Rydberg state by light from pulsed dye lasers and by multiphoton microwave absorption. They then drifted approximately 15 cm to a time-resolved detector which was sensitive only to the  $n = 22$  atoms. The drift time was chosen to be close to the free space radiative lifetime. Thus, the time-of-flight spectrum was the product of the probability density for the Maxwell-Boltzmann velocity distribution of the atomic beam and the exponential decay curve for spontaneous emission. To assure accuracy of the method, the free space lifetime was compared to the theoretical result and was found to agree within the experimental resolution, approximately 2%.

Next, the drift space was modified by the introduction of two parallel conducting plates separated by the distance  $d = \lambda/2$ . The plates behaved effectively as waveguide at cutoff. It can be shown that in this situation the decay rate switches abruptly from zero to a value slightly greater than the free space value as the cutoff separation is exceeded. In the experiment the plate separation was kept fixed and the wavelength was slightly varied by the Stark effect in an applied electric field.

Figure 22.3 shows the experimental time-of-flight curves on either side of cutoff. The area under the curves is proportional to the total number of atoms that reached the detector. The most conspicuous effect of inhibited spontaneous emission is the great increase in area. However, the shape of the curve also contains information about the lifetime. In the inhibited region the lifetime was determined to be at least 20 times larger than the free space value.



Inhibited spontaneous emission offers the possibility of increasing the resolution of spectroscopic measurements beyond the limit set by the natural lifetime. The experiment has also achieved significantly longer time-of-flight times than previously possible with Rydberg atoms, providing a useful technical advance toward high resolution millimeter wave spectroscopy.

## 22.2.2 Rydberg Atoms in Cavities

Thomas Gentile, Barbara Hughey, Daniel Kleppner

We are carrying out a study of single Rydberg atoms radiating into a single mode of the radiation field at a temperature which is effectively zero. Work is in progress on designing the beam and preparing the cavity.

### References

- <sup>1</sup> Kleppner, D., Phys. Rev. Lett. *47*, 223 (1981).
- <sup>2</sup> Hulet, R.G., E. Hilfer, D. Kleppner, Phys. Rev. Lett. *55*, 2137, (1985).
- <sup>3</sup> Hulet, R.G., and D. Kleppner, Phys. Rev. Lett. *51*, 1430 (1983).

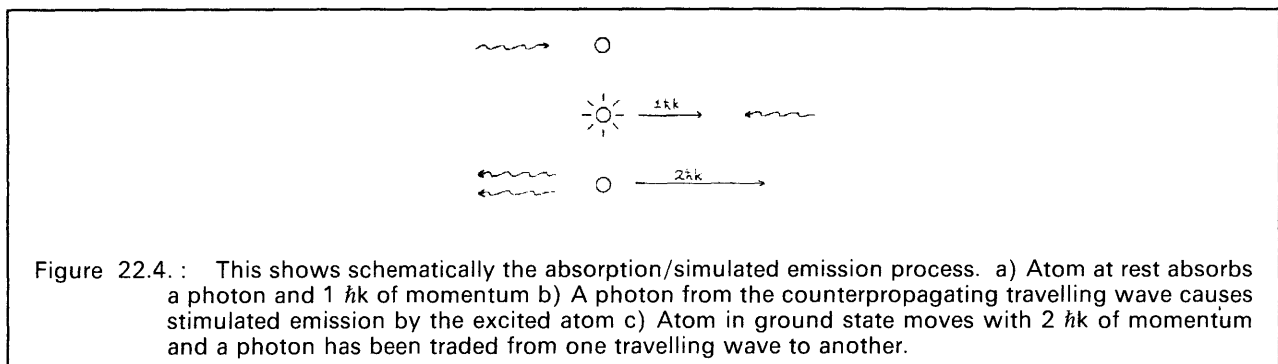
## 22.3 Experimental Study of Momentum Transfer to Atoms by Light

*National Science Foundation (Grant PHY 86-05893)*

Peter J. Martin, Bruce G. Oldaker, Andrew H. Miklich, Jacques Derouard, David E. Pritchard

We are investigating the radiative forces experienced by a two-level atom interacting with light. These forces provide a new way to study the fundamental interaction between atoms and radiation, and also have important implications in the slowing, cooling and trapping of neutral atoms using light.

By deflecting a highly collimated (0.7  $\hbar k$  FWHM resolution), state-selected, and velocity selected 11% FWHM) atomic sodium beam with a well-characterized light wave, we are able to make quantitative measurements of many aspects of momentum transfer to atoms by light. Our apparatus is the only one in the world capable of quantitative comparison with a single photon resolution.



Emphasis this year has been on momentum transfer by a standing wave. Here the momentum transfer can be viewed in terms of a classical force (the dipole force) which arises from the interaction of the induced electric dipole moment with the gradient of the standing-wave electric field. If the laser is detuned far enough from resonance, spontaneous emission is negligible and the process can be described by a semi-classical Hamiltonian. The momentum transfer can also be described as absorption/stimulated emission of photon pairs from the two counterpropagating traveling waves which make up the standing wave (see Fig. 22.4), a view which predicts momentum transfer in discrete units of  $2 \hbar k$  as we observed. If the standing wave is considered as a diffraction grating,  $2 \hbar k$  is the reciprocal lattice vector in which momentum must be transferred if the grating is not excited.

The latest results concerned the force on a moving atom. If the atom initially has a non-zero velocity component,  $v_{||}$ , along the  $\vec{k}$ -vector of the standing wave, then the two counterpropagating waves appear to be Doppler shifted, one by  $+kv_{||}$  and the other by  $-kv_{||}$ . This Doppler shift leads to a dephasing of the absorption/stimulated emission process and a predictable reduction in the momentum transfer to the atom. Figure 22.5 shows typical data of the momentum transfer for three different velocities,

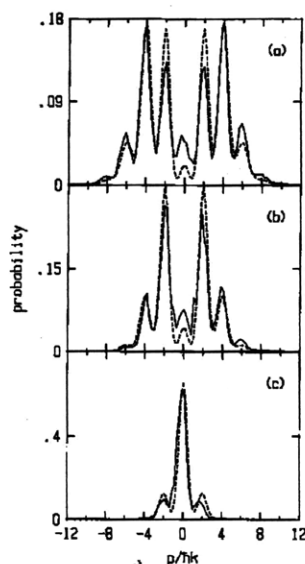


Figure 22.5. : Diffraction patterns of atomic sodium from a standing light wave for different initial velocities of the sodium atom along the  $\vec{k}$ -vector of the standing wave. a)  $v_{||} = -1.2$  m/sec b)  $v_{||} = -0.77$  m/sec c)  $v_{||} = 1.5$  m/sec. Dashed line is theoretical prediction convolved with measured experimental resolution.

$v_{||}$ .<sup>1</sup> The dashed lines are predictions for this case which we obtained from a fully quantum mechanical theory which we derived this year.

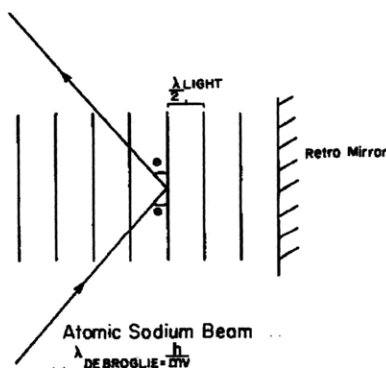
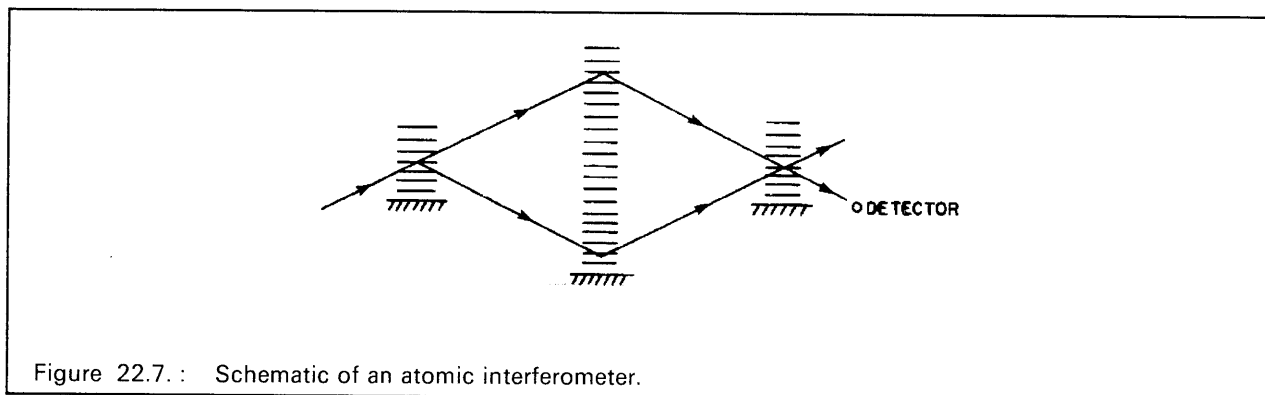


Figure 22.6. : Schematic of Bragg scattering of an atomic atomic sodium wave off a standing light wave.

Another breakthrough this year has been the observation of Bragg scattering of atomic waves off a standing wave light “crystal.” If the atomic beam is viewed as a plane wave and the antinodes of the standing wave define crystal planes, then large resonances for momentum transfer occur for incident angles,  $\theta$ , satisfying the Bragg law,

$$2d\sin\theta = n\lambda_{D.B.}, \text{ where } d = \frac{\lambda_{light}}{2}, \lambda_{D.B.} = \frac{h}{mv}$$

is the deBroglie wavelength of the atomic wave, and  $n$  is an integer (see Fig. 22.6).<sup>2</sup>



Evidence of this new phenomenon opens up new possibilities for the construction of an “atomic interferometer”; which is basically a device that interferes atomic waves. Figure 22.7 shows schematically such a device. The “atomic beam splitter” uses Bragg scattering to split the atomic beam coherently. The “atomic mirror” again uses Bragg scattering to steer the two beams to the last “atomic beam splitter” which recombines the two beams. If the effective path length of one of the two legs of the interferometer is modulated (for example, by the use of an electric field), there will be a modulation of the relative phases of the two recombined beams and intensity modulation at the detector. Besides the point of showing complete duality of particles and waves, this device can be used to measure the polarizability of the atoms, the phase shift produced by passage through a gas, the light shift, and possibly the Casimir shift. The Casimir shift arises because the lowest order modes of the vacuum fluctuations are excluded from the region between two parallel conducting plates due to electromagnetic boundary conditions at the plates. If one of the paths of the interferometer passes through this region, then there will be less of an energy shift of the ground state of the atoms on this path of the interferometer, and hence a phase shift at the detector.

## References

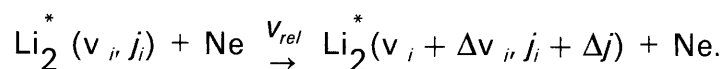
- <sup>1</sup> P.J. Martin, P.L. Gould, B.G. Oldaker, and A.H. Miklich, accepted for publication in *Phys. Rev. A*.
- <sup>2</sup> A.F. Bernhardt, and B.W. Shore, *Phys. Rev. A*. 23, 1290 (1981).

## 22.4 Atom-Molecule Collisions

*National Science Foundation (Grant ECS 84-21392)*

Brien Stewart, Peter Magill, Richard Stoner, Jacques Derouard, David E. Pritchard

What happens when an atom collides with a rapidly rotating, vibrating molecule? The answer to this question is emerging in a detailed experimental study of vibrationally inelastic (VRI) collisions in our laboratory.<sup>1,2,3,4,5</sup> The subject of our study is the atom-diatom system



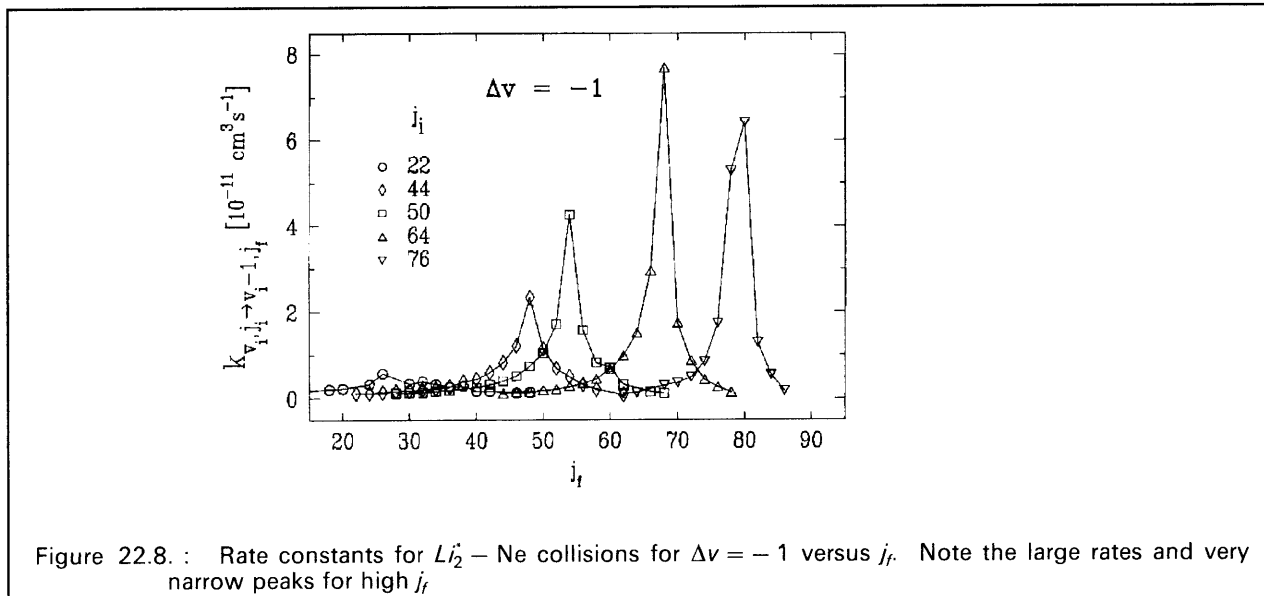
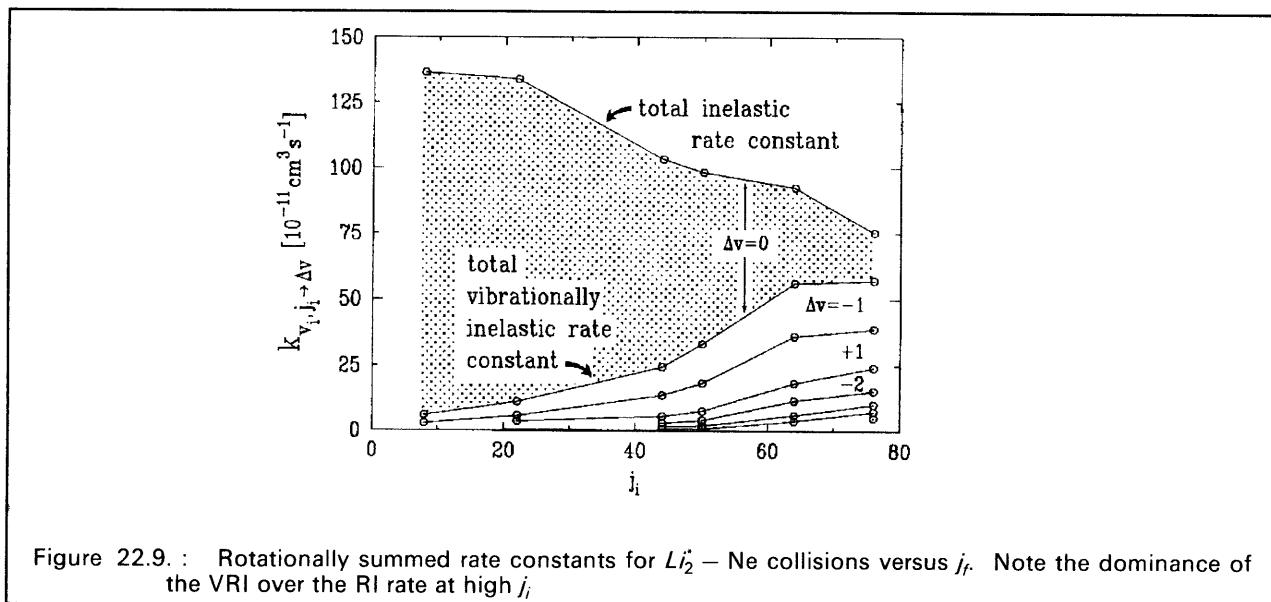


Figure 22.8. : Rate constants for  $Li_2 - Ne$  collisions for  $\Delta v = -1$  versus  $j_f$ . Note the large rates and very narrow peaks for high  $j_f$ .

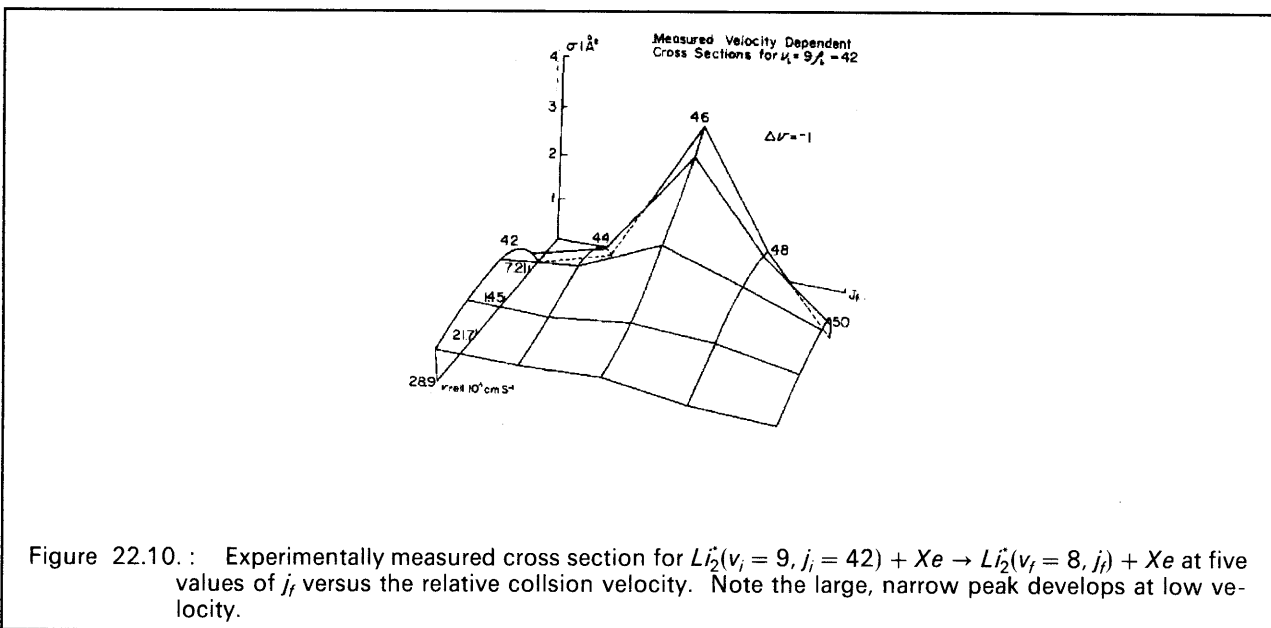
We use single mode tunable dye lasers to select the initial vibrational ( $v_i$ ) and rotational ( $j_i$ ) levels of the  $Li_2$  molecule; in addition, we can select the collision velocity via the Doppler shift. Our investigation has uncovered a new type of vibrationally inelastic collision process: at high  $j_i$  the VRI cross section becomes very large, but with a very narrow  $j_f$  distribution for a given  $\Delta v$ . In addition, the peak of this distribution is correlated with  $\Delta v$  according to the rule  $\Delta j = -4\Delta v$ .

Figure 22.8 shows experimental rate constants for  $\Delta v = -1$  and  $j_i$  ranging from 22 to 76. Note the large, sharply peaked rate constants at large  $j_i$ ; the largest of these corresponds to a level-to-level cross section of  $8\text{\AA}^2$ . At  $j_i = 64$ , the width of the  $j_f$  distribution is only  $3\hbar$ . This resonance-like behavior has prompted us to name the phenomenon “quasi-resonant  $V \leftrightarrow R$  transfer,” quasi-resonant, because the peak of the  $j_f$  distribution is not determined by internal energy conservation, that is, by a simple interconversion of vibrational and rotational energy.

Inelastic rates summed over  $j_f$  are shown in Figure 22.9, illustrating that VRI collisions are the dominant inelastic process at high  $j_i$ . At the highest  $j_i$  measured, the quasi-resonant  $V \leftrightarrow R$  rate accounts for more than  $2/3$  of the total inelastic rate. This is a complete reversal of what occurs at low  $j_i$ , the regime of essentially all previous studies. At low  $j_i$ , VRI rates are much smaller than purely rotational inelastic (RI) rates and have broad, unspecific  $j_f$  distributions, as can be seen in the  $j_i = 22$  data of Figure 22.8.



At sub-thermal velocities, the quasi-resonant process is strengthened further. Figure 22.10 shows velocity dependent cross sections measured by our VSDS (Velocity Selection via the Doppler Shift) technique.<sup>6</sup> The cross section and final state specificity are increased by lowering the velocity. Again, this behavior is exactly the opposite of what is observed at low  $j_i$ , where increases in velocity *enhance* vibrational inelasticity.



We have modeled quasi-resonant  $V \leftrightarrow R$  transfer using classical trajectories calculated by a technique that allows us to follow the time dependence of the vibrational action (corresponding to the vibrational quantum number).<sup>7</sup> Examination of many trajectories has enabled us to describe the dynamics of the quasi-resonant process and characterize the conditions under which it occurs.<sup>3</sup> At low  $j_i$ , the force on the vibrator is largely averaged out by the molecular oscillation, which induces much more rapid changes in the intermo-

lecular potential than either the rotation or translation; the result is little change in the vibration. At high  $j_i$ , the molecule rotates substantially during a vibrational period, yielding a sudden force on the vibrator that can produce large changes in the vibration. The correlation of  $\Delta v$  and  $\Delta j$  results from a subtle interaction of the vibrational and rotational phases at the instant of maximum force. Finally, at very low velocity, the molecule can collide several times with the atom due to the rapid rotation, resulting in an enhancement in the above effects and a strengthening of  $V \leftrightarrow R$  transfer. Each of these effects can be seen in Figure 22.11, a plot of some of the dynamical variables versus time through one collision. The top two graphs (of  $v$  and  $j$ ) show that at each step through the collision  $\Delta v$  and  $\Delta j$  are anti-correlated and that each "collisionette" of an end of the molecule with the atom builds on the others, resulting in a large net transfer.

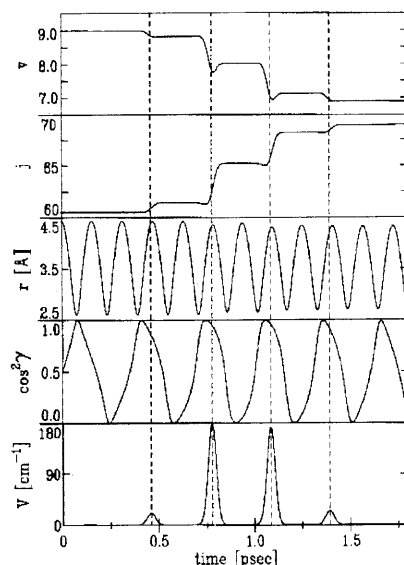


Figure 22.11. : Plot of the vibrational action ( $v$ ), the rotational action ( $j$ ), the internuclear separation ( $r$ ), cosine of the rotational angle ( $\gamma$ ) and the intermolecular interaction energy ( $V$ ) as functions of time through a single, simple collision. Note the peaks in  $V(t)$  corresponding to "collisionettes."

Because this model has been successful, we can use it to make predictions about as yet unobserved classical effects. A good example of such an effect is the collisional reorientation of the molecular rotation axis. For collisions which are either rotationally inelastic or not, the *direction* of the angular momentum vector  $\vec{j}$  can be altered. Utilizing the polarization of the incident and fluorescent light, the reorientation cross section can be measured experimentally. Classical trajectory calculations can readily make predictions about the amount of reorientation and the cross section for it. In addition, trajectories naturally give the velocity dependence of this process which can also be measured experimentally using the Doppler shift.

## References

- <sup>1</sup> K.L. Saenger, N. Smith, S.L. Dexheimer, C. Engelke, and D.E. Pritchard, J. Chem. Phys. 79, 4076 (1983).
- <sup>2</sup> T. Scott, Ph.D. Thesis, M.I.T., Cambridge, Mass., 1985.

- <sup>3</sup> P. Magill, T. Scott, B. Stewart, N. Smith, and D.E. Pritchard, to be submitted to J. Chem. Phys.
- <sup>4</sup> T. Scott, B. Stewart, P. Magill, N. Smith, and D.E. Pritchard, to be submitted to J. Chem. Phys.
- <sup>5</sup> B. Stewart, P. Magill, T.P. Scott, J. Derouad, and D.E. Pritchard, to be submitted to Phys. Rev. Lett. Lett.
- <sup>6</sup> N. Smith, T. Scott, D.E. Pritchard, J. Chem. Phys. *81*, 1229 (1984).
- <sup>7</sup> N. Smith, J. Chem. Phys. *85*, 1987, (1986).
- <sup>8</sup> P. Magill, B. Stewart, D.E. Pritchard, to be submitted to Phys. Rev. Lett.

## 22.5 Magnetic Trapping of Neutral Atoms

*U.S. Navy - Office of Naval Research (Contract N00014-83-K-0695)*

Vanderlei Bagnato, Gregory Lafyatis, Alexander Martin, Eric Raab, Riyadh Ahmad-Bitar, David E. Pritchard

We are working on a program to slow, trap and cool neutral atoms. Laser light is used to slow and cool atoms and magnetic forces are used to trap them. Ultimately we hope to be able to trap atoms for days and cool them to temperatures on the order of  $10^{-6}$ K. In addition to the interesting scientific and technical challenges involved in trapping and cooling atoms, we hope to open several new lines of investigation with these cooled atoms. Cold trapped atoms constitute a good system for studying collective phenomena such as Bose condensation, low energy - Na and Na - Na<sup>+</sup>, and coherent optical effects (the deBroglie wavelength can exceed the optical wavelength). They also offer opportunities for performing ultra-high resolution spectroscopy and are extremely promising candidates for a new generation of frequency standards.

In 1986 we completed construction of our neutral trap apparatus and began doing experiments with it. Our first successful run has advanced the state of the neutral atom slowing and trapping art by several orders of magnitude. We have continuously stopped atoms with laser light, continuously loaded them into our 0.1K deep superconducting magnetic trap, and held them for up to six minutes. Continuous trap loading is an important advance over previous pulsed loading <sup>1</sup> schemes because it permits the accumulation of large numbers of atoms in the trap and, hopefully, enables the study of collective phenomena in the trap. Our trap, though somewhat more complicated in design and construction than the two previously reported atom traps <sup>2</sup> has the advantage of a uniform magnetic field region in its center in which optical pumping and precision spectroscopy of cooled atoms may be undertaken. Fluorescence from trapped atoms has been observed for 10 sec with intense illumination. Finally, we have observed trapping decay times of two minutes -- two orders of magnitude better than the previously reported traps. It is our expectation that we will soon see trapping times of hours, or perhaps days, giving us sufficient time to perform experiments on the trapped atoms. We are now in a position to

move neutral traps from the status of laboratory curiosities to that of powerful tools for new research in physics.

Figure 22.12 is a schematic of our experiment. Superconducting magnets were designed and constructed to provide the necessary field to slow and trap neutral atoms. Na atoms from a 500°C oven are slowed, in two stages, by laser beams propagating counter to the atomic beam. A tapered magnetic field creates a Zeeman shift in the atomic levels and compensates for the changing Doppler shift of the atoms as they slow. The second laser beam is retroflected and cools the atoms to milliKelvin temperatures near the trap's center. We trap atoms in states whose electron spin is parallel to the magnetic field -- these atoms experience a force towards regions of weak field (c.f. Stern-Gerlach experiment). The field minimum located at the center of our trapping magnets constitutes a 0.12K deep trap for atoms. Photodiodes located at several places within the apparatus are used to detect fluorescence from the slowing and trapped atoms.

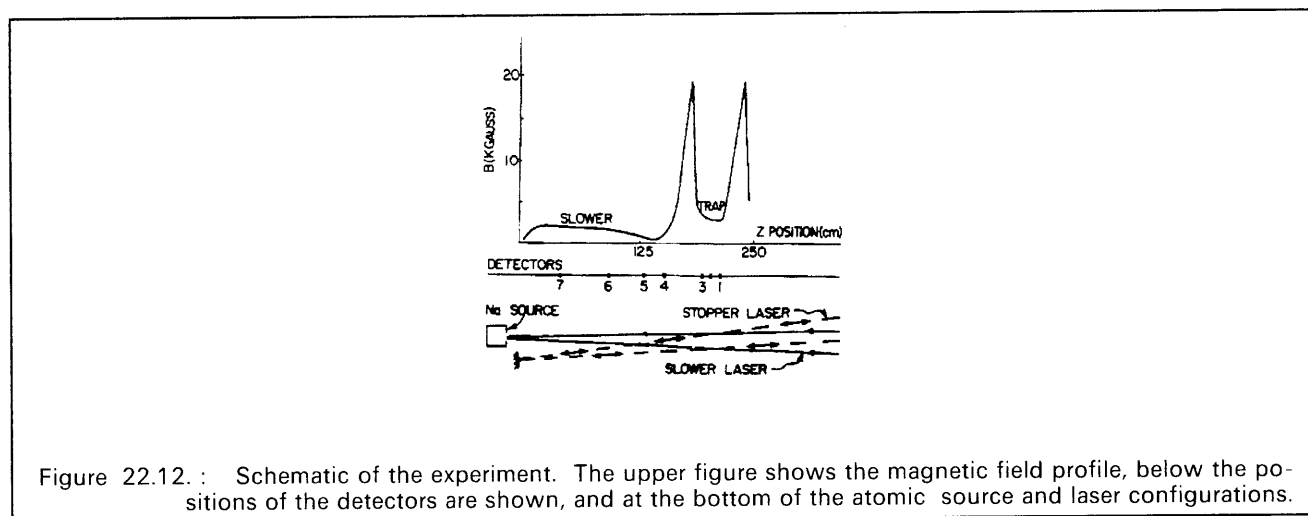


Figure 22.13 is a composite of several runs in which the trap lifetime was measured by recording the fluorescence from trapped atoms. The sequence used to make up Figure 22.13 was: lasers on to fill the trap, lasers off for a (variable) period of time, second laser turned back on to probe the remaining atoms. Our diagnostics for those initial measurements were coarse and presently we can only make a lower limit estimate in the number of atoms in the trap:  $\approx 10^8$ . There may well be two orders of magnitude more trapped atoms which have inadvertently decayed to another hyperfine state which is well out of resonance with the laser light. This inadvertent optical pumping should enable us to perform RF resonance on the trapped atoms. In the future we hope to accumulate more atoms, study Doppler cooling of the trapped atoms (expected to achieve submilliKelvin temperatures), investigate "cyclic" cooling of atoms<sup>3</sup> (projected to achieve temperatures near  $1\mu\text{K}$ ) and use RF resonance both to study the trapped atoms and possibly to develop a frequency standard.

## References

- <sup>1</sup> Migdall, A. et. al., Phys. Rev. Lett. 54, 2595 (1985).
- <sup>2</sup> Chu, S., J.E. Bjorkholm, A. Ashkin, Cable, Phys. Rev. Lett. 27, 314 (1986).

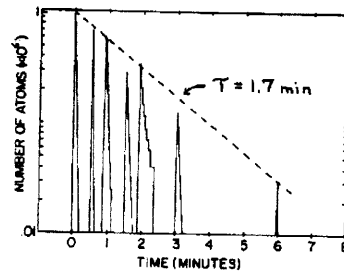


Figure 22.13. : Result of several runs. Each curve is the result of charging the trap, blocking both laser beams, and after the indicated time, turning back on the stopping beam and recording the fluorescence from trapped atoms.

<sup>3</sup> Pritchard, D.E., Phys. Rev. Lett. *51*, 1336 (1983).

## 22.6 Precision Mass Spectroscopy of Ions

*National Science Foundation (Grant CHE 84-21392)*

*Joint Services Electronics Program (Contract DAALO3-86-K-0002)*

Eric Cornell, Robert W. Flanagan, Greg P. Lafyatis, David E. Pritchard, Robert M. Weisskoff

We are developing an experiment to determine the mass of individual atomic and molecular ions at precisions of  $10^{-11}$ . This technique will allow us to do a variety of experiments which address issues of both fundamental and applied physics:

- The  ${}^3\text{H}^+ - {}^3\text{H}_e^+$  mass difference is an important parameter in ongoing experiments to measure the electron neutrino rest mass.
- Excitation and binding energies of typical atomic and molecular ions might be studied by “weighing” the small increase in energy:  $\Delta m = E_{\text{bind}} / c^2$ .
- Experiments that weigh  $\gamma$ -rays can be used in a new method to determine  $N_A$ , the Avogadro constant.
- Traditional applications of mass spectroscopy should benefit from the several orders of magnitude improvement in both accuracy and sensitivity our approach offers over conventional techniques.

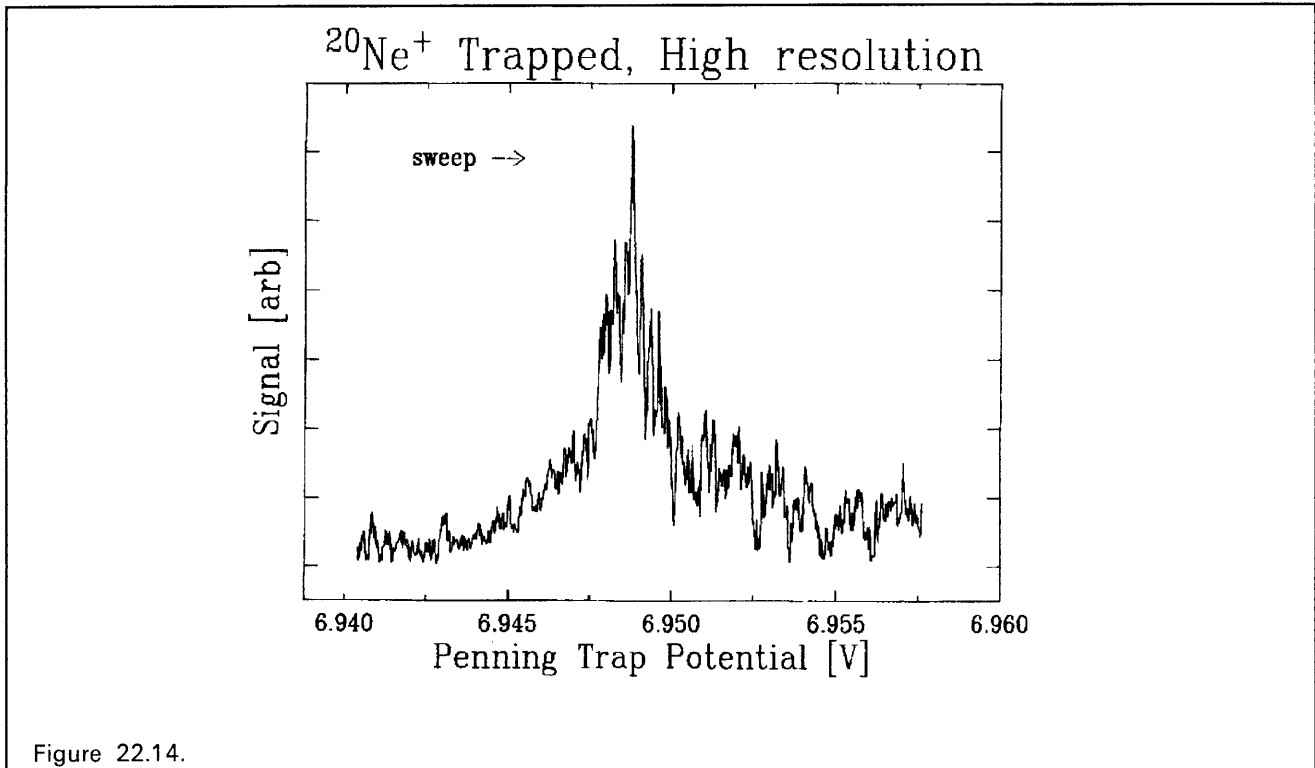


Figure 22.14.

We will measure ratios of cyclotron frequencies, and, therefore, masses of a small number of atomic or molecular ions in a Penning trap at 4.2K. To attain the precision we seek, it will be necessary to work with only one, or at most, two ions in the trap. Space charge from other ions would lead to undesirable frequency shifts. Thus, our mass spectrometer will have the ultimate sensitivity -- a single particle.

We will use ion trapping techniques based on methods developed at the University of Washington, where they have made precision measurements on protons, electrons and positrons at the  $10^{-11}$  level. Trapped ions are detected by the small currents which they induce in the trap electrodes as they move. However, because atomic and molecular ions have larger masses, and thus lower resonant frequencies, they induce much smaller currents than the particles studied at Washington. Consequently, much of our past effort has been to develop a detector using a SQUID (Superconducting QUantum Interference Device) and superconducting electronics to measure these small induced currents, typically  $\sim 3 \times 10^{-15} \text{A}$ .

This year we assembled our apparatus and began making measurements with the short term goal of detecting and manipulating single ions. Although we have detected many species,  $^{20}\text{Ne}^+$  has proved a convenient species to work with. To date, we have been able to observe clouds of fewer than five ions. Figure 22.14 is a typical observation of an ion cloud, which is driven resonantly by voltages applied to the trap. In Figure 22.15, we turned off the drives and observed the ions oscillating incoherently in the trap, measured with a fourier transform of the endcap currents. We also have made multiply charged species by leaving on the electron gun (below the trap) and further ionizing already trapped ions. Figure 22.15 is a broad scan in which we detected  $\text{Ne}^+$ ,  $\text{Ne}^{2+}$ ,  $\text{Ne}^{3+}$ , and  $\text{Ne}^{4+}$  made in that manner.

In the coming year we hope to observe single ions and begin cyclotron resonance work.

